Biosensors and Bioelectronics 33 (2012) 247–253

Contents lists available at SciVerse ScienceDirect

Biosensors and Bioelectronics

journal homepage: www.elsevier.com/locate/bios

Electrochemical determination of microRNA-21 based on graphene, LNA integrated molecular beacon, AuNPs and biotin multifunctional bio bar codes and enzymatic assay system

Huanshun Yin[a,1], Yunlei Zhou[b,1], Haixia Zhang[a], Xiaomeng Meng[a], Shiyun Ai[a,*]

[a] College of Chemistry and Material Science, Shandong Agricultural University, Taian, 271018, Shandong, China
[b] College of Life Science, Beijing Normal University, 100875, Beijing, China

ARTICLE INFO

Article history:
Received 6 October 2011
Received in revised form 9 January 2012
Accepted 13 January 2012
Available online 23 January 2012

Keywords:
MicroRNA-21
Graphene
Dendritic gold nanoparticles
Locked nucleic acid
Hairpin molecule beacon
Electrochemical biosensor

ABSTRACT

MicroRNAs (miRNAs), a kind of small, endogenous, noncoding RNAs (~22 nucleotides), might play a crucial role in early cancer diagnose due to its abnormal expression in many solid tumors. As a result, label-free and PCR-amplification-free assay for miRNAs is of great significance. In this work, a highly sensitive biosensor for sequence specific miRNA-21 detection without miRNA-21 labeling and enrichment was constructed based on the substrate electrode of dendritic gold nanostructure (DenAu) and graphene nanosheets modified glassy carbon electrode. Sulfydryl functionalized locked nucleic acid (LNA) integrated hairpin molecule beacon (MB) probe was used as miRNA-21 capture probe. After hybridized with miRNA-21 and reported DNA loading in gold nanoparticles (AuNPs) and biotin multi-functionalized bio bar codes, streptavidin–HRP was brought to the electrode through the specific interaction with biotin to catalyze the chemical oxidation of hydroquinone by H_2O_2 to form benzoquinone. The electrochemical reduction signal of benzoquinone was utilized to monitor the miRNA-21 hybridization event. The effect of experimental variables on the amperometric response was investigated and optimized. Based on the specific confirmation of probe and signal amplification, the biosensor showed excellent selectivity and high sensitivity with low detection limit of 0.06 pM. Successful attempts are made in miRNA-21 expression analysis of human hepatocarcinoma BEL-7402 cells and normal human hepatic L02 cells.

1. Introduction

MicroRNAs (miRNAs) are small, endogenous, noncoding RNAs (~22 nucleotides) found in diverse organisms, which play crucial roles in cell proliferation, differentiation and apoptosis. Up to date, 1426 miRNAs have been identified in the human genome. Recent researches have shown that abnormal expression of miRNAs is associated with a variety of human cancers (Esquela-Kerscher and Slack, 2006). Among various miRNAs, miRNA-21 has been identified as the only miRNA over-expressed in 11 types of solid tumors, including stomach, prostate, head and neck, esophagus, glioblastoma, neuroblastoma, cholangiocarcinoma, breast, lung, colorectal, and pancreatic cancer (Lu et al., 2008; Medina and Slack, 2008). Therefore, miRNA-21 could be potential biomarkers for clinical diagnosis. In order to understand the functions of miRNA-21 in diseases diagnosis, there is an urgent need to develop reliable and ultrasensitive methods for miRNA-21 determination.

At the present time, miRNA-21 is detected with techniques such as Northern blot (Kim et al., 2010), in situ hybridization (Yamamichi et al., 2009), RT-PCR (Huang et al., 2009), microarrays (Yan et al., 2008) and bioluminescence assay (Cissell et al., 2008). Although Northern blot and in situ hybridization are used as the standard methods, these detection approaches have low sensitivity and generally require many steps, resulting laborious time-consuming procedures that are difficult for routine miRNA analysis (Catuogno et al., 2011). RT-PCR can only be used to quantify miRNA precursors rather than the mature miRNAs expression, because the low detection selectivity and nonlinear target amplification might distort gene expression. Microarray needs fluorescent dyes labeled with miRNA target sequences to characterize the hybridization event, which might quench from the excitation light or from environment effects and require expensive instrument. Direct hybridization of miRNA samples onto the microarray requires a large amount of total RNA (Castoldi et al., 2008). Moreover, northern blot, RT-PCR and microarray need expensive commercial kits. Bioluminescence

* Corresponding author. Tel.: +86 538 8247660; fax: +86 538 8242251.
E-mail address: ashy@sdau.edu.cn (S. Ai).
[1] These two authors contributed equally to this work.

0956-5663/$ – see front matter © 2012 Elsevier B.V. All rights reserved.
doi:10.1016/j.bios.2012.01.014

assay needs to label and enrich miRNAs. In addition, it requires trivial operation, expensive instruments and reagents.

To enhance the sensitivity, improve the selectivity, and make the detection limit and cost low, electrochemical biosensors based on signal amplification have been investigated to detect miRNAs due to their high sensitivity and selectivity, low detection limit, low cost, and ease of automatization (Drummond et al., 2003). For instances, Gao's group developed a series of sensitive electrochemical biosensors for monitoring miRNAs hybridization based on miRNAs labeled with $Os(dmpy)_2(IN)Cl^+$ (Gao and Yu, 2007b), $Ru(PD)_2Cl_2Os$ (Gao and Yu, 2007a), OsO_2 nanoparticles (Gao and Yang, 2006) and RuO_2 nanoparticles (Peng and Gao, 2011; Peng et al., 2010), respectively. Though the detection limit can be achieved to 800, 200, 80, 3 and 2 fM, respectively, this kind of monitor methods need to enrich and label miRNAs, which will increase the operation complicacy because of the low abundance of miRNAs in real samples. For decreasing influence of tagging and enriching miRNAs, and achieving the direct detection of miRNA in real sample, Kelly's group utilized electrostatic interaction between miRNA and $Ru(NH_3)_6^{3+}$ and the electrocatalytic effect between $Ru(NH_3)_6^{2+/3+}$ and $Fe(CN)_6^{4-/3-}$, a detection limit as low as 10 aM was achieved with a limited dynamic range of 10^2 (Yang et al., 2009). Lusi et al. (2009) exploited a simple and fast label-free electrochemical genosensor for miRNAs detection based on guanine oxidation consequent to the hybrid formation between the microRNA and its inosine substitute capture probe. Pöhlmann and Sprinzl (2010) developed a rapid, selective, and sensitive gap hybridization assay for detection of mature miRNAs without label based on four components DNA/RNA hybridization and electrochemical detection using esterase 2-oligodeoxynucleotide conjugates with the detection limit of 2 aM. All of these detection techniques showed high sensitivity, efficiency and selectivity, indicating that electrochemical biosensors can be alternative to other detection techniques.

In this work, we described a sensitive and selective miRNA biosensor based on graphene and dendritic gold nanostructure (DenAu) modified glassy carbon electrode (GCE), LNA integrated molecular beacon probe, multifunctional encoded DNA–AuNPs–LNA bio bar codes and HRP catalysis signal amplification, in which, the molecular beacon was not labeled with fluorescent and quencher groups, only a —SH was labeled at its 5′-end for assembly on the electrode surface. DNA–Au bio bar codes have become increasingly incorporated bioassays with its effective amplification based on AuNPs functionalized with a large number of oligonucleotide strands. Different from previous reports, the AuNPs were labeled with two oligonucleotide strands. One is LNA integrated DNA, which was complementary to the 3′-end of molecular beacon probe. The other is biotin functionalized DNA, not complementary to probe. The length of the probe (41 bases) was longer than the target miRNA (22 bases). The 5′-end of the molecular (5′–3′, No. 6–27 bases) was complementary to miRNA and its 3′-end (5′–3′, No. 28–41 bases) was complementary to LNA integrated DNA in DNA–AuNPs–LNA bio bar codes. After hybridization with target miRNA, the stem-loop structure of molecular beacon was unfolded and its 3′-end was forced far away from the electrode surface to hybridize with LNA integrated DNA. Then, with specific interaction between biotin and streptavidin, the streptavidin functionlized horseradish peroxidase (streptavidin–HRP) can be immobilized on the electrode surface to catalyze the oxidation reaction of hydroquinone by H_2O_2 to form benzoquinone and enhance the electrochemical reduction signal of benzoquinone (Chen et al., 2011; Laczka et al., 2011; Zhang et al., 2011). The detection strategy was shown in Scheme 1. Taking advantage of tri-amplification effects of the DenAu/graphene/GCE, multifunctional encoded AuNP and HRP, the biosensor showed high determination sensitivity for miRNA with detection limit of 0.06 pM (S/N = 3).

2. Experimental

2.1. Materials and apparatus

All oligonucleotides were synthesized and HPLC-purified by TaKaRa Biotechnology Co., Ltd. (Dalian, China), and their sequences are shown as follows, LNA integrated molecular beacon probe: 5′-SH—$(CH_2)_6$-GGC CGT CAA **C**AT CAG TC**T** GAT AAG C**T**A AAC ATG ATA CGG CC-3′; target miRNA-21 (S1), 5′-UAG CUU AUC AGA CUG AUG UUG A-3′; single-based mismatch miRNA, 5′-UAG CUU AUC ***G***GA CUG AUG UUG A-3′; three-based mismatch miRNA, 5′-U***U***G CUU AUC ***G***GA CUG AU***C*** UUG A-3′; non-complementary miRNA, 5′-GUA AGG CAU CUG ACC GAA GGC A-3′; LNA integrated reported DNA (S2), 5′-SH—$(CH_2)_6$-GG**C** **C**GT A**T**C ATG T**T**-3′; signal DNA (S3), 5′-SH—$(CH_2)_6$-GCG GAA CAC TCA AG-3′-biotin (nucleotide mismatches were indicated as italic and bold letters, locked nucleic acid bases were indicated as underlined and bold letters, the complementary section for probe to target miRNA-21 was indicated as bold letters with shade.). Synthetic DNA and miRNA sequences were dissolved in DEPC treated Milli-Q water with autoclaved sterilization and kept frozen. Graphene was synthesized according to previous report (Li and Wu, 2009). AuNPs were synthesized according to previous reports by chemical reduction using sodium citrate as reductant (Liu and Lu, 2006). Streptavidin labeled horseradish peroxidase (streptavidin–HRP), polyethylene glycol 3350 (PEG-3350) and ethidium bromide (EB) were purchased from Sigma (USA). Streptavidin–HRP was diluted 100 times with 10 mM phosphate buffer solution (PBS, pH 7.0). TRIzol reagent was from Invitrogen (USA). Diethypyrocarbonate (DEPC) was from Solarbio (China). Mercaptopropanoic acid (MPA), tri(2-carboxyethyl) phosphine hydrochloride (TCEP), tris(hydroxymethyl)aminomethane (Tris), disodium ethylenediaminetetraacetic acid (EDTA), sodium citrate, chloroauric acid and polyethylene glycol 3350 (PEG-3350) were purchased from Aladdin (Shanghai, China). All reagents were analytically pure grade.

The buffer solutions employed in this study are as follows. Probe immobilization buffer: 10 mM Tris–HCl, 1.0 mM EDTA, 1.0 M NaCl, and 1.0 mM TCEP (pH 7.0), miRNA hybridization buffer: 1 × SSC, DNA hybridization buffer: 10 mM Tris–HCl, 1.0 mM EDTA, and 1.0 M NaCl (pH 7.0), electrochemistry determination buffer, 0.1 M PBS (pH 7.0). All reagents were analytically pure grade. All of the solution and redistilled deionized water used were treated with DEPC and autoclaved to protect from RNase degradation.

Electrochemical experiments were performed with CHI660C electrochemical workstation (USA) with a conventional three-electrode cell. A bare GCE or modified GCE was used as working electrode. A saturated calomel electrode (SCE) and a platinum wire were used as the reference electrode and auxiliary electrode, respectively. Transmission electron microscopy (TEM) image was taken with JEOL-1200EX instrument (Japan). Atomic force microscopy (AFM) measurement was performed on Digital Instruments MultiMode (USA). RNA concentration and quality were assessed spectrophotometrically at 260 and 280 nm using NanoVue TM equipment (GE-Healthcare, Buckinghamshire, UK). All the measurements were carried out at room temperature (25 ± 0.5 °C).

2.2. Preparation of bio bar coded gold nanoparticles

The preparation of multifunctional encoded DNA–AuNPs bio bar codes was performed according to previous report with minor revision (Hu et al., 2008). In brief, the mixture of 5.0×10^{-10} mol of LNA integrated reported DNA and 2.0×10^{-9} mol of signal DNA was activated with acetate buffer (pH 5.2) and 1.5 μL of 10 mM TCEP for 1 h, then added to 1 mL of freshly prepared gold nanoparticles synthesized by chemical reduction, and shaken gently for 24 h. Then, the DNA–AuNPs conjugates were aged in salts (0.1 M NaCl, 10 mM

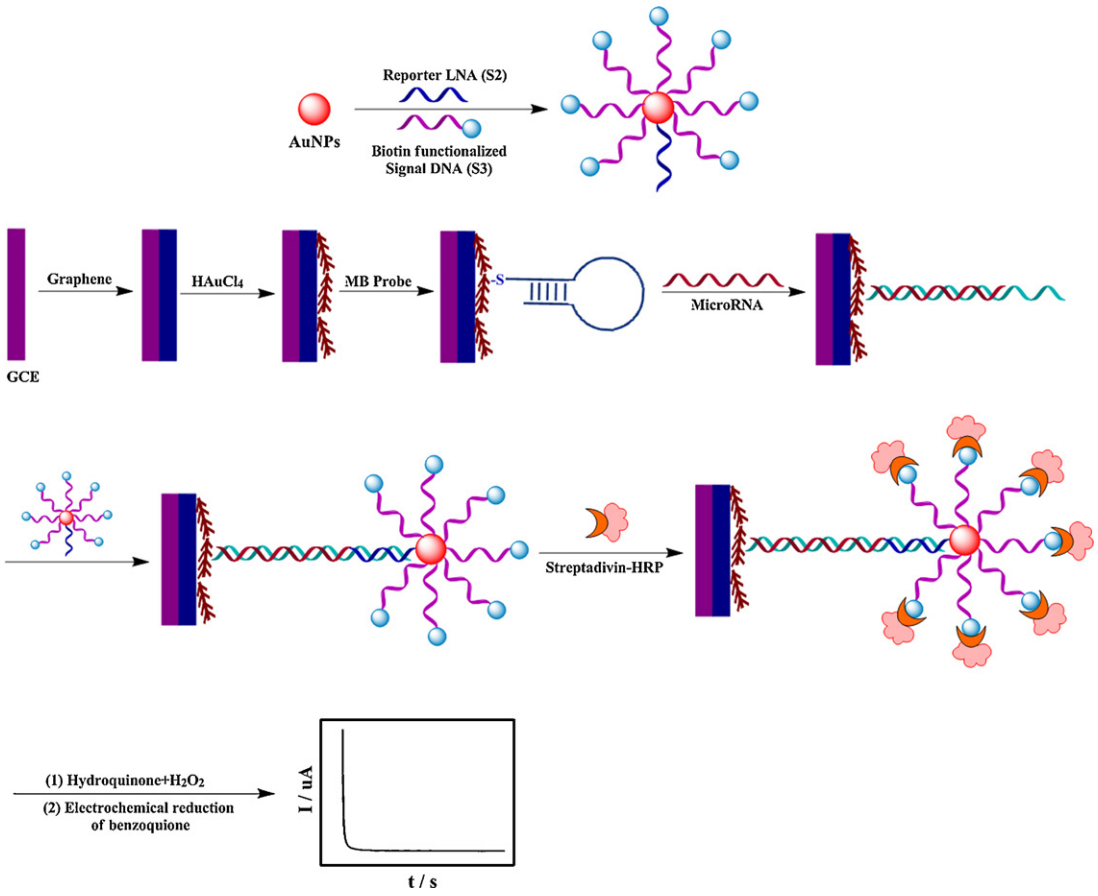

Scheme 1. Chronoamperometry determination of microRNA hybridization through three steps of amplification.

acetate buffer) for another 24 h. Excess reagents were removed by centrifuging at 12,000 rpm for 30 min. The red precipitate was washed and centrifuged repeatedly for three times. The resulting nanoparticles were dispersed into a buffer solution (pH 8.2) and stored at 4 °C.

2.3. Preparation of DenAu/graphene/GCE

The GCE was polished with 0.03 μm alumina powder on microcloth pad and rinsed thoroughly with redistilled deionized water. Then the polished electrode was washed successively with redistilled deionized water, anhydrous ethanol and redistilled deionized water in an ultrasonic bath. After dried with nitrogen blowing, 5 μL of graphene dispersion (2 mg/mL) was dripped on the electrode surface and dried under infrared lamp. After washed with redistilled deionized water, the electrode was immersed into 3 mM $HAuCl_4$ solution containing 0.1 M KNO_3 and the DenAu were electrochemically deposited on the electrode surface by single-potential mode using amperometry *i–t* technique at −0.2 V for 900 s (Ding et al., 2010). Finally, the electrode was washed with redistilled deionized water and dried with room temperature. The obtained electrode was noted as DenAu/graphene/GCE.

2.4. Probe immobilization and hybridization

For avoiding the formation of dipolymer, the molecular beacon probe was treated subsequently at 70 °C water bath for 30 min and ice-cold water bath for 10 min before immobilization (Mao et al., 2008). The DenAu/graphene/GCE was immersed into an immobilization buffer solution containing 1.0×10^{-8} M probe and 5.0×10^{-8} M MPA for 24 h to obtain a well-aligned probe monolayer, followed by rinsed three times with washing buffer (10 mM Tris–HCl, pH 7.0) to remove the unspecific adsorbed probe molecule and MPA. Hybridization reaction between the immobilized probe and target miRNA-21 was carried out by immersing the modified electrode into hybridization buffer containing a certain concentration of miRNA-21 for 2.5 h at room temperature in a humidified chamber. After that, the electrode was rinsed three times with 0.1 × SSC for 15 min to remove the un-hybridized target miRNA-21 (the obtained electrode was noted as MiRNA-Probe/DenAu/graphene/GCE). The MiRNA-Probe/DenAu/graphene/GCE was secondly hybridized with reporter probes loaded on AuNPs for 2 h at room temperature. After hybridization, the electrode was extensively rinsed with washing buffer (10 mM Tris–HCl, pH 7.0) and dried under a stream of nitrogen (the obtained electrode was noted as bio-bar-codes/MiRNA-Probe/DenAu/graphene/GCE).

2.5. Streptavidin–HRP covalent binded with biotin

The bio-bar-codes/MiRNA-Probe/AuNPs/graphene/GCE was incubated in 0.05% PEG-3350 solution (prepared in 0.1 M PBS) for 1.5 h to prevent any possible nonspecific binding. After the electrode was rinsed three times with 0.1 M PBS (pH 7.0) for 5 min, 8 μL streptavidin–HRP (1:100) was dropped on the electrode surface and incubated for 30 min at room temperature. The electrode was then rinsed three times with 0.01 M PBS and dried with room temperature. The obtained electrode was noted as HRP/bio-bar-codes/MiRNA-Probe/DenAu/graphene/GCE.

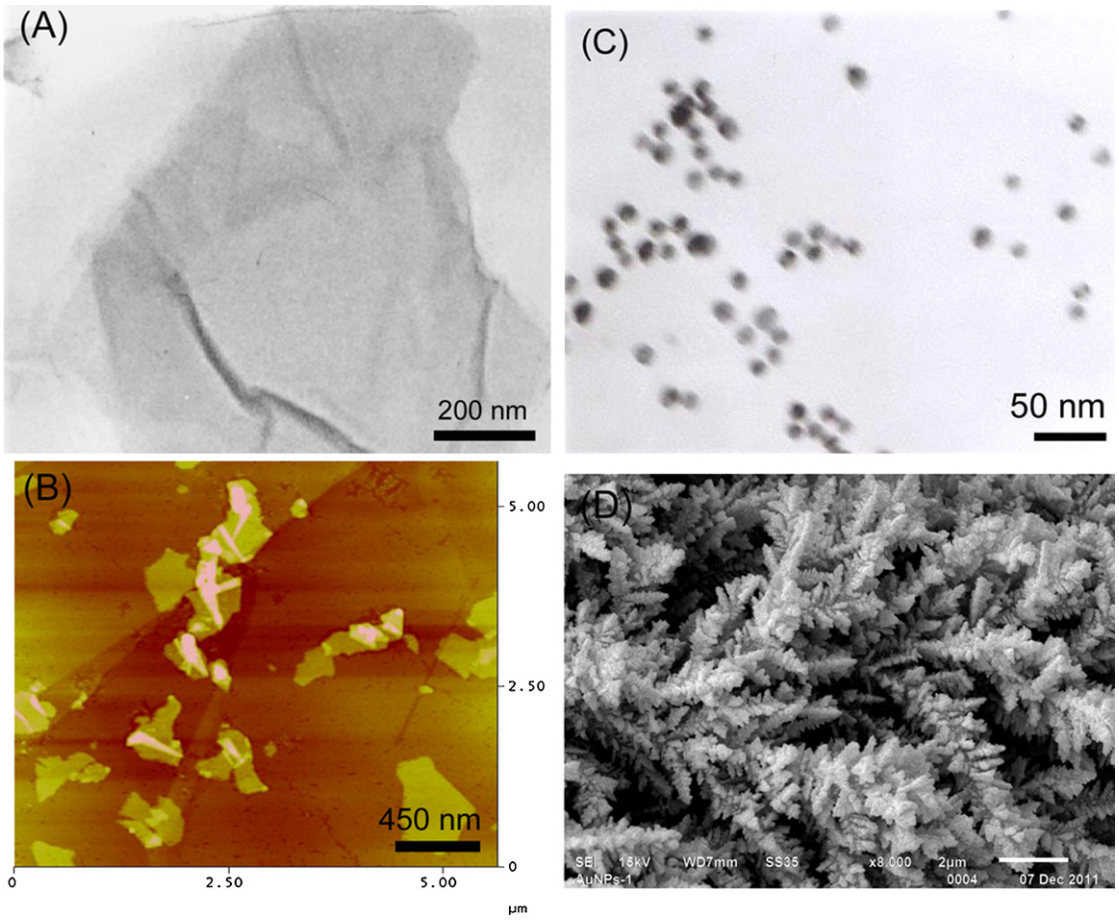

Fig. 1. TEM images of graphene (A) and AuNPs (C); AFM images of graphene (B) and DenAu/graphene/GCE (D).

2.6. Electrochemical determination

Cyclic voltammetry (CV) and chronoamperometry (CA) was performed in 10 mL of 0.1 M PBS (pH 7.0) containing 0.1 mM H_2O_2 and 0.2 mM hydroquinone with the applied potential of −0.2 V for CA and a scan rate of 100 mV/s in the potential range from −0.5 to 0.6 V for CV, respectively.

2.7. Total RNA extraction

Human hepatocarcinoma BeL-7402 cells and normal human hepatic L02 cells were obtained from College of life science, Beijing Normal University (China). Cells were cultured in Dulbecco's modified Eagle's medium (DMEM, purchase from GIBICO, USA) containing 10% fetal calf serum (FCS) (Invitrogen, New Zealand) at 37 °C in the presence of 5% CO_2. Total RNA from the cells was extracted using TRIzol reagent according to the manufacturer's recommended protocol. RNA concentration was determined by UV–vis spectrophotometry. RNA integrity was checked by TBE agarose gel electrophoresis.

3. Results and discussion

3.1. Characterization of graphene, AuNPs and DenAu

The synthesized graphene were characterized by TEM and AFM. As can be seen in Fig. 1A, graphene showed the crumpled and wrinkled flake-like structure, which can increase the electrode effective surface. Fig. 1B shows the AFM image of graphene, only individual flat graphene with thickness of 2.3 nm was observed. This height is larger than the value predicted by theory, indicating the few layer graphene sheets (Schniepp et al., 2006). This phenomenon can attribute the individual graphitic sheets bearing oxygen-containing groups on both faces. Fig. 1C presents the TEM image of AuNPs. The image indicated that the AuNPs obtained were spherical and the average size was about 13 nm. The SEM image of DenAu/graphene/GCE was shown in Fig. 1D, which proved that Au with symmetrical dendritic structure was successfully immobilized on electrode by electrochemical deposition. From this image, it can also be observed that the symmetrical dendritic structure was composed of AuNPs, which was in accordance with previous report by electrodepositing AuNPs at −1.4 V for 600 s (Li et al., 2011). This symmetrical dendritic structure can greatly increase the electrode effective surface area and improve the probe immobilization amount, which were proved by the following investigations.

3.2. Electrode characterization

Electrochemical impedance spectroscopy (EIS) is a useful technique to monitor the impedance changes of the electrode surface during the modification process. The semicircle diameters of Nyquist plot at high frequency region reflect the electron transfer resistance (R_{et}), which is from the electron transfer of the redox probe $[Fe(CN)_6]^{3-/4-}$ (Zhu et al., 2010). Fig. 2 shows the EIS results of different electrodes in $[Fe(CN)_6]^{3-/4-}$ solution with the frequencies swept from 10^{-1} to 10^5 Hz. The R_{et} of the bare GCE was 682 Ω (curve a). Graphene/GCE (curve b) and DenAu/graphene/GCE (curve c) exhibited an almost straight line, which was just the characteristic of the diffusional limiting step of the electrochemical process, indicating that graphene and DenAu can increase the electrode

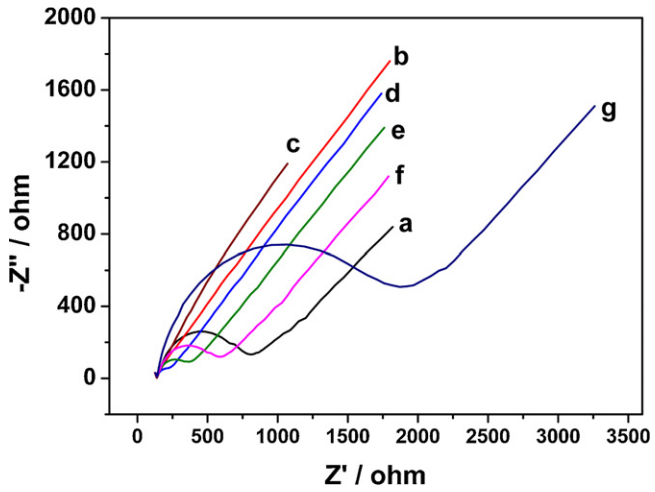

Fig. 2. Nyquist plots of different electrode in 5 mM $Fe(CN)_6^{3-/4-}$ containing 0.1 M KCl. (a) GCE, (b) graphene/GCE, (c) DenAu/graphene/GCE, (d) Probe/DenAu/graphene/GCE, (e) MiRNA-Probe/DenAu/graphene/GCE, (f) bio-bar-codes/MiRNA-Probe/DenAu/graphene/GCE and (g) HRP/bio-bar-codes/MiRNA-Probe/DenAu/graphene/GCE.

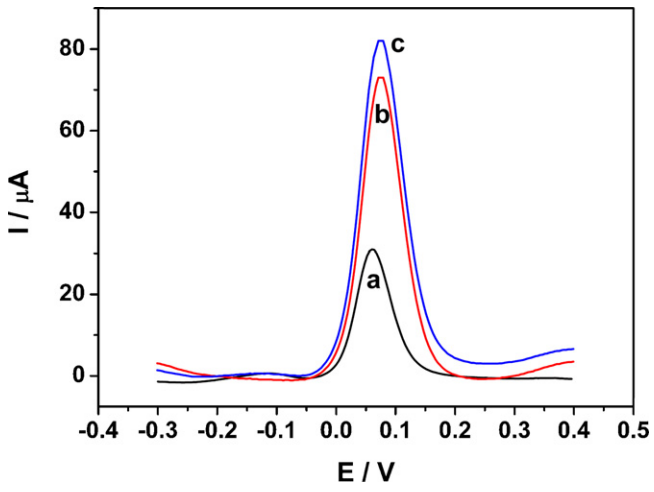

Fig. 3. Differential pulse voltammograms of HRP/bio-bar-codes/MiRNA-Probe/DenAu/GCE (a), and HRP/bio-bar-codes/MiRNA-Probe/DenAu/graphene/GCE (b and c) in 0.1 M PBS (pH 7.0) containing 0.1 mM H_2O_2 and 0.2 mM hydroquinone after background subtraction. MiRNA-21 hybridization concentration, 1×10^{-8} (a and b) and 1×10^{-7} M (c).

conductivity and facilitate the electron transfer from the redox probes to electrode surface. In addition, DenAu can further increase the effective electrode surface area and thus have the potential to anchor more DNA probes to amplify the signal. After assembling probe and MCH, a small semi-circle at high frequency region was observed and the R_{et} value was 89.1 Ω (curve d). The increase in R_{et} was due to the immobilization of negatively charged phosphoric acid backbone of molecular beacon probe repels the negatively charged $Fe(CN)_6^{3-/4-}$ and inhibit the electron transfer. After the probe hybridized with target miRNA-21 (curve e), the R_{et} value increased to 245.2 Ω. Subsequently, the value of R_{et} increased to 461.1 Ω when the un-hybridized fragment of probe hybridized with LNA integrated reported DNA (S2) loaded on the AuNPs, due to the large amount of DNA and LNA linked on the AuNPs (curve f). After the electrode was sealed with PEG-3350 and specific interacted with streptavidin–HRP (curve g), the R_{et} value increased significantly (1795 Ω), due to the increase of the thickness of the interface. The phenomenon was consistent with the fact that the protein layer was insulated and blocked the interfacial electron transfer. This was the direct evidence of successful binding of enzyme on the electrode surface.

Because the aim of this work is determine miRNA-21 based on signal amplification using LNA integrated molecular beacon probe, the probe immobilization amount can direct influence the determination sensitivity. Thus, we immobilized the probe onto DenAu modified graphene/GCE, not DenAu/GCE. The reason can be attributed to two aspects. One is that graphene possesses excellent conductivity, which can increase the electrochemical response of benzoquinone. The other is that graphene has high specific surface area and can increase the electrode effective surface area, so more DenAu can be electrochemically deposited on the electrode surface to assemble more probe molecules. For confirming it, the electrode effective surface area was determined based on the reduction peak area of gold oxide when the electrode was immersed in 0.5 M H_2SO_4 and scanned from 0 to 1.6 V by cyclic voltammetry (Fig. S1 in supplementary material). The reduction peak areas were 2.843 and 6.104 mC for DenAu/GCE and DenAu/graphene/GCE, respectively. According to previous report (Trasatti and Petrii, 1991), the specific charge of gold oxide reduction can be assumed to be 386 μC/cm^2. Therefore, the active surface area of DenAu/graphene/GCE can be calculated to be 15.81 cm^2, while the corresponding DenAu/GCE was 7.36 cm^2. It was clear that the electrode effective area was increased.

For confirming that graphene and DenAu can improve the determination sensitivity of the proposed method, the electrochemical behavior of the fabricated biosensor was investigated in 0.1 M PBS (pH 7.0) containing 0.1 mM H_2O_2 and 0.2 mM hydroquinone by differential pulse voltammetry (Fig. 3). The reduction peak current of HRP/bio-bar-codes/MiRNA-Probe/DenAu/graphene/GCE (curve b) was higher than that at HRP/bio-bar-codes/MiRNA-Probe/DenAu/GCE (curve a) after background subtraction, which can be attributed to the good conductivity of graphene and DenAu. Graphene can not only increase the reduction peak current, but also increase the electrode area to immobilize more DenAu. The increased DenAu can increase the reduction peak current. More importantly, the increased DenAu can immobilized more probes on the electrode surface, then more AuNPs functionalized bio bar codes and HRP can be immobilized on the electrode surface. When the hybridization concentration of miRNA-21 increased (curve c), the reduction peak current of benzoquinone also increased. Therefore, we thought that the developed method can be applied to monitor miRNA-21 hybridization event.

3.3. Optimization of experimental conditions

Because the high hybridization efficiency can improve the determination sensitivity and discriminate specific sequence, the effect of probe concentration, probe immobilization time, miRNA-21 hybridization time and reported DNA hybridization time on the reduction peak current of benzoquinone was investigated by chronoamperometry.

Fig. S2A (supplementary material) shows the influence of probe concentration on miRNA-21 hybridization. The reduction signal of benzoquinone increased with probe concentration increasing from 10^{-11} to 10^{-8} M and the maximum current was obtained at 10^{-8} M. With increasing the molecular beacon probe concentration, more probes can be immobilized on the electrode. However, too many probes on the electrode surface can lead to the difficulty in unfolding the loop-stem structure of probe to hybridize with target miRNA-21 due to the steric hindrance effect. Therefore, 10^{-8} M prone concentration was selected. Fig. S2B (supplementary material) shows the effect of probe immobilization time on the on the reduction current of benzoquinone. The current

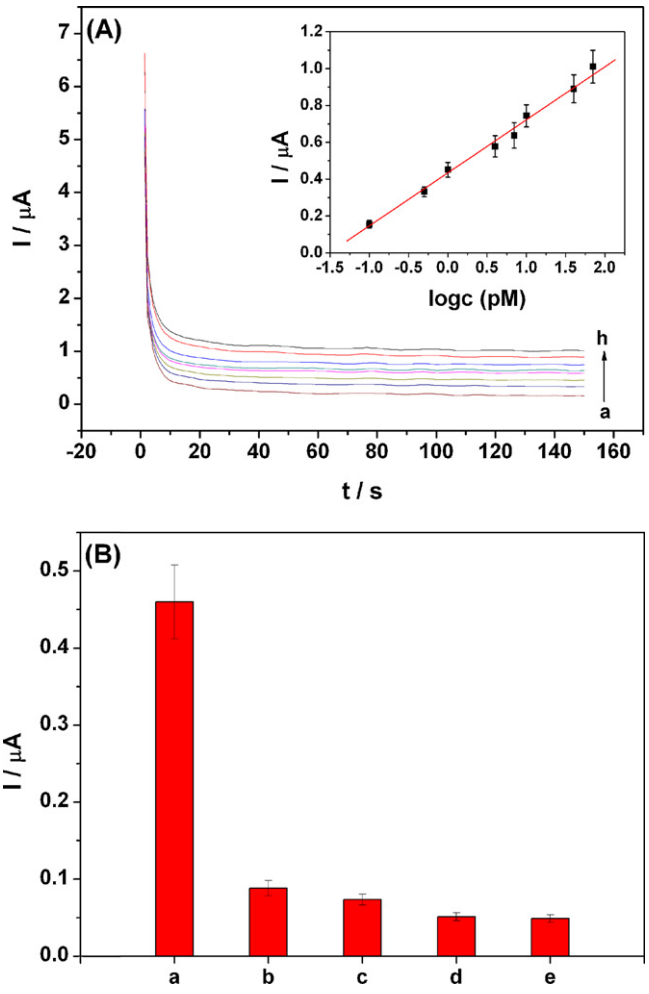

Fig. 4. (A) Amperometric responses for the biosensor with probe hybridized with target miRNA-21 at different concentrations. (a–h) 0.1, 0.5, 1, 4, 7, 10, 40 and 70 pM; insert: calibration curve. (B) Comparison of amperometric signal of the biosensor after hybridization with target miRNA-21 (a), single-base mismatched miRNA (b), three-base mismatched miRNA (c) and non-complementary miRNA (d) after background subtraction. MiRNA concentration, 1 pM.

increased gradually with extending the immobilization time from 12 to 24 h. Then the current decreased reversely. Considering the determination sensitivity, 24 h was selected as the optimal condition. The effect of hybridization time was investigated by hybridizing with target miRNA-21 with probe from 30 to 180 min (Fig. S3C in supplementary material). With the time increasing from 30 to 120 min, the reduction current increased gradually. Then, the current increased very slightly with further extending the hybridization time. To ensure the relative high hybridization and determination efficiency, 120 min was selected throughout our experiments. Fig. S2D (supplementary material) shows the effect of hybridization time of the reported DNA loaded on AuNPs with probe on the reduction current of benzoquinone. Similar to miRNA-21, the current increased gradually from 30 to 150 min, and then the increase tendency slowed down. Therefore, 150 min was selected as the optimum hybridization time.

3.4. Detection sensitivity and selectivity for miRNA-21

Chronoamperometry is an electrochemical technique that has been widely applied to monitor DNA–DNA or DNA–miRNA hybridization events (Gao and Yang, 2006; Pöhlmann and Sprinzl, 2010; Wang et al., 2011). Therefore, chronoamperometry was performed to examine the detection sensitivity of the biosensor after hybridization with the target miRNA-21 at different concentrations. As can be seen in Fig. 4A, the current increased linearly with the increasing target miRNA-21 concentration ranging from 0.1 to 70 pM. The regression equation can be expressed as $I = 0.29 \log c + 0.43$ ($R = 0.9956$) and the detection limit was estimated to be 0.06 pM.

Four kinds of miRNA sequences including the complementary target miRNA-21, the single-base mismatch miRNA, the four-base mismatch miRNA, and the non-complementary miRNA were chosen to study the selectivity. Fig. 4B shows the comparison of the currents of these four miRNA sequences with same concentration (1 pM) hybridized with probe and the background. Among the four kinds of miRNA sequences, the current of complementary target miRNA-21 was 0.46 μA (column a), which was much higher than those of the other mismatch sequences with the currents of 0.088 μA (single-base mismatch, column b), 0.074 μA (three-base mismatch, column c), and 0.051 μA (non-complementary, column d), respectively. The blank background current was 0.049 μA (column e). These results demonstrated that the biosensor was able to discriminate complementary target miRNA-21 as the target with high specificity and sensitivity.

Besides sensitivity and selectivity, reproducibility is also extremely important feature for biosensors in the practical application such as clinical diagnoses. To investigate it, six electrodes were fabricated independently at the same conditions and used to detect miRNA-21 (1 pM). The relative standard deviation (RSD) was 10.05%, which was comparable with previous reports (Gao and Yang, 2006; Gao and Yu, 2007c; Lusi et al., 2009; Pöhlmann and Sprinzl, 2010). This result indicated that the proposed biosensor has acceptable reproducibility for miRNA-21 determination considering the instability and low abundance of miRNA-21.

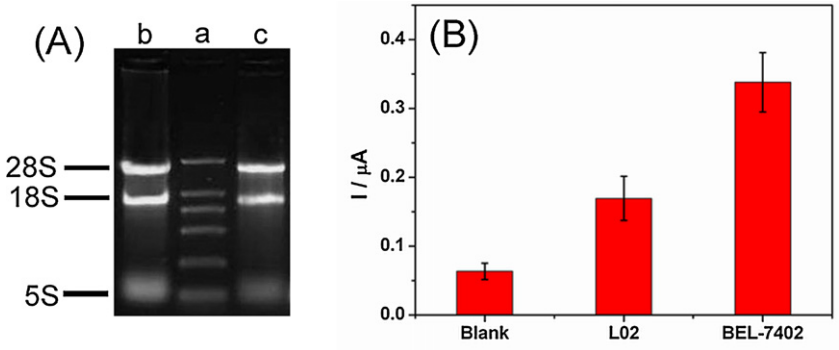

Fig. 5. (A) 1% agarose gel electrophoresis of isolated total RNA. (a) DNA marker, (b) human hepatocarcinoma BEL-7402 cells and (c) normal human hepatic L02 cells. (B) Electrochemical responses of the biosensor after hybridization with extract total RNA samples.

3.5. Expression analysis of miRNA-21 in cells

With the high sensitivity and selectivity, the biosensor allowed us to directly and PCR-freely analyze miRNA expression in total RNA extracted from cells. Because hepatocarcinoma is the most common malignancy of the liver, the fifth most common cancer worldwide, and the third most common cause of cancer deaths (Liu et al., 2010), we measured the electrochemical response after hybridization with miRNA-21 in diluted total RNA extracted from human hepatocarcinoma BEL-7402 cells and normal human hepatic L02 cells. The integrity of the total RNA was confirmed by agarose gel electrophoresis (Fig. 5A). The three bands of 28S, 18S and 5S were obtained, indicating the integrity of total RNA. The ratio of A_{260} and A_{280} was 1.789 and 1.681 for L02 cells and BEL-7402 cells, respectively, implying the relative high purity of total RNA. As can be seen in Fig. 5B, after hybridization with a total RNA sample extracted from BEL-7402 cells, a significant electrochemical signal was generated compared with that at L02 cells, indicating that the expression level of miRNA-21 in BEL-7402 cells was up-regulated, which was in accordance with previous report (Selaru et al., 2009). In fact, the concentrations of miRNA-21 in L02 and BEL-7402 cells were 0.127 and 0.489 pM. The relative errors were 11.83% and 12.98% for BEL-7402 and L02 cells, respectively. Thus, this biosensor can offer a satisfactory accuracy in the direct identification of differentially expressed miRNAs in cells.

4. Conclusions

In summary, we developed an electrochemical biosensor for direct detection miRNA-21 hybridization in real samples without label and enrichment based on triple signal amplification. First, the graphene and DenAu were immobilized onto the substrate GCE to improve the conductivity and electrochemical effective surface area, through which the immobilization amount of capture LNA integrated molecular beacon probe was enhanced. Second, AuNPs functionalized DNA bio bar codes hybridized with 3′-end of probe to increase the immobilization amount of biotin. Third, streptavidin–HRP specifically interacted with biotin to amplify the electrochemical response of benzoquinone. Based on these amplifications, the detection limit of 0.06 pM was achieved. The biosensor showed excellent selectivity for different miRNA sequences. This strategy can also be applied as efficient tools for rapid, specific and direct detection of extremely low concentration of other miRNA.

Acknowledgements

This work was supported by the National Natural Science Foundation of China (No. 21075078, 21105056) and the Natural Science Foundation of Shandong province, China (No. ZR2010BM005, ZR2011BQ001).

Appendix A. Supplementary data

Supplementary data associated with this article can be found, in the online version, at doi:10.1016/j.bios.2012.01.014.

References

Castoldi, M., Schmidt, S., Benes, S., Hentze, M.W., Muckenthaler, M.U., 2008. Nat. Protoc. 3 (2), 321–329.
Catuogno, S., Esposito, C.L., Quintavalle, C., Cerchia, L., Condorelli, G., de Franciscis, V., 2011. Cancers 3 (2), 1877–1898.
Chen, X., Chen, Z., Zhu, J., Xu, C., Yan, W., Yao, C., 2011. Bioelectrochemistry 82 (2), 87–94.
Cissell, K.A., Rahimi, Y., Shrestha, S., Hunt, E.A., Deo, S.K., 2008. Anal. Chem. 80 (7), 2319–2325.
Ding, C., Wang, Z., Zhong, H., Zhang, S., 2010. Biosens. Bioelectron. 25 (5), 1082–1087.
Drummond, T.G., Hill, M.G., Barton, J.K., 2003. Nat. Biotechnol. 21 (10), 1192–1199.
Esquela-Kerscher, A., Slack, F.J., 2006. Nat. Rev. Cancer 6, 259–269.
Gao, Z., Yang, Z., 2006. Anal. Chem. 78 (5), 1470–1477.
Gao, Z., Yu, Y., 2007a. Biosens. Bioelectron. 22 (6), 933–940.
Gao, Z., Yu, Y., 2007b. Sens. Actuators B 121 (2), 552–559.
Gao, Z., Yu, Y.H., 2007c. Biosens. Bioelectron. 22 (6), 933–940.
Hu, K., Lan, D., Li, X., Zhang, S., 2008. Anal. Chem. 80 (23), 9124–9130.
Huang, G.L., Zhang, X.H., Guo, G.L., Huang, K.T., Yang, K.Y., 2009. Oncol. Rep. 21 (3), 673–679.
Kim, S.W., Li, Z., Moore, P.S., Monaghan, A.P., Chang, Y., Nichols, M., John, B., 2010. Nucleic Acids Res. 38 (7), e98.
Laczka, O., Maesa, J.-M., Godino, N., del Campo, J., Fougt-Hansen, M., Kutter, J.P., Snakenborg, D., Muñoz-Pascual, F.-X., Baldrich, E., 2011. Biosens. Bioelectron. 26 (8), 3633–3640.
Li, F., Han, X., Liu, S., 2011. Biosens. Bioelectron. 26 (5), 2619–2625.
Li, Y., Wu, Y., 2009. J. Am. Chem. Soc. 131 (16), 5851–5857.
Liu, C., Yu, J., Yu, S., Lavker, R.M., Cai, L., Liu, W., Yang, K., He, X., Chen, S., 2010. J. Hepatol. 53 (1), 98–107.
Liu, J., Lu, Y., 2006. Nat. Protoc. 1 (1), 246–252.
Lu, Z., Liu, M., Stribinskis, V., Klinge, C.M., Ramos, K.S., Colburn, N.H., Li, Y., 2008. Oncogene 27 (31), 4373–4379.
Lusi, E., Passamano, M., Guarascio, P., Scarpa, A., Schiavo, L., 2009. Anal. Chem. 81 (7), 2819–2822.
Mao, X., Jiang, J., Xu, X., Chu, X., Luo, Y., Shen, G., Yu, R., 2008. Biosens. Bioelectron. 23 (10), 1555–1561.
Medina, P.P., Slack, F.J., 2008. Cell Cycle 7 (16), 2485–2492.
Pöhlmann, C., Sprinzl, M., 2010. Anal. Chem. 82 (11), 4434–4440.
Peng, Y., Gao, Z., 2011. Anal. Chem. 82 (3), 820–827.
Peng, Y., Yi, G., Gao, Z., 2010. Chem. Commun. 46 (48), 9131–9133.
Schniepp, H.C., Li, J.L., McAllister, M.J., Sai, H., Herrera-Alonso, M., Adamson, D.H., Prud'homme, R.K., Car, R., Saville, D.A., Aksay, I.A., 2006. J. Phys. Chem. B 110 (17), 8535–8539.
Selaru, F.M., Olaru, A.V., Kan, T., David, S., Cheng, Y., Mori, Y., Yang, J., Paun, B., Jin, Z., Agarwal, R., Hamilton, J.P., Abraham, J., Georgiades, C., Alvarez, H., Vivekanandan, P., Yu, W., Maitra, A., Torbenson, M., Thuluvath, P.J., Gores, G.J., LaRusso, N.F., Hruban, R., Meltzer, S.J., 2009. Hepatology 49 (5), 1595–1601.
Trasatti, S., Petrii, O., 1991. Pure Appl. Chem. 63 (5), 711–734.
Wang, K., Sun, Z., Feng, M., Liu, A., Yang, S., Chen, Y., Lin, X., 2011. Biosens. Bioelectron. 26 (6), 2870–2876.
Yamamichi, N., Shimomura, R., Inada, K.-I., Sakurai, K., Haraguchi, T., Ozaki, Y., Fujita, S., Mizutani, T., Furukawa, C., Fujishiro, M., Ichinose, M., Shiogama, K., Tsutsumi, Y., Omata, M., Iba, H., 2009. Clin. Cancer Res. 15 (12), 4009–4016.
Yan, L.-X., Huang, X.-F., Shao, Q., Huang, M.-Y., Deng, L., Wu, Q.-L., Zeng, Y.-X., Shao, J.-Y., 2008. RNA 14 (11), 2348–2360.
Yang, H., Hui, A., Pampalakis, G., Soleymani, L., Liu, F.-F., Sargent, E.H., Kelley, S.O., 2009. Angew. Chem. Int. Ed. 48 (45), 8461–8464.
Zhang, Z., Tang, A., Liao, S., Chen, P., Wu, Z., Shen, G., Yu, R., 2011. Biosens. Bioelectron. 26 (7), 3320–3324.
Zhu, Z., Li, X., Zeng, Y., Sun, W., 2010. Biosens. Bioelectron. 25 (10), 2313–2317.